

A Tucker Decomposition Based Approach for Topographic Functional Connectivity State Summarization

Arash Mahyari, Selin Aviyente

Department of Electrical and Computer Engineering
Michigan State University

Outline

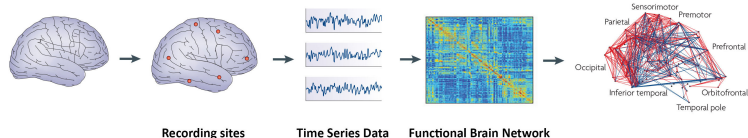
- 1 Introduction
- 2 Time-Frequency Phase Synchrony
- 3 Tensor Subspace Analysis
- 4 State Representation
 - Subject Summarization
 - Time Summarization
- 5 Experimental Results
- 6 Conclusion and Future Work

Outline

- 1 **Introduction**
- 2 **Time-Frequency Phase Synchrony**
- 3 **Tensor Subspace Analysis**
- 4 **State Representation**
 - Subject Summarization
 - Time Summarization
- 5 **Experimental Results**
- 6 **Conclusion and Future Work**

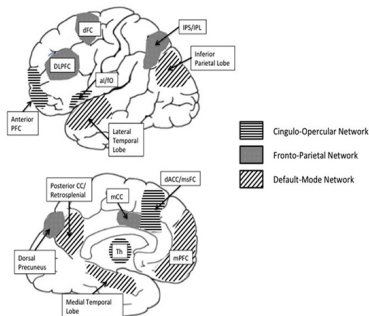
Introduction

- Higher brain functions depend on the balance between local specialization (functional segregation) and global integration (functional integration) of brain processes (Friston, 2011; Friston, 2001; Le Van Quyen, 2003; Stam, 2005; Tononi et al., 1998).
- Imaging neuroscience (EEG, MEG, fMRI) has firmly established functional segregation as a principle of brain organization in humans.
- The integration of segregated areas has proven more difficult to assess.
- Therefore, there is a need to identify task-related interactions between neuronal populations.



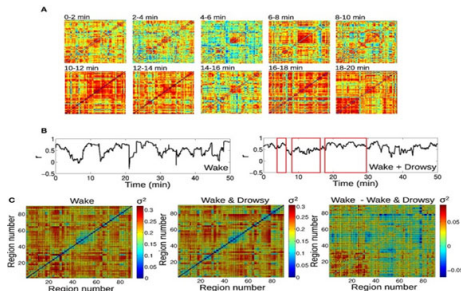
Functional Connectivity

- Cognitive control processes are responsible for goal or context representation and maintenance, attention allocation and stimulus-response mapping.
- In particular, for cognitive control:
 - ▶ Medial prefrontal cortex (mPFC) and lateral prefrontal cortex (IPFC) play an important role.
 - ▶ Synchronization connects anterior cingulate cortex (ACC) and IPFC (Womelsdorf et al. 2014, Current Biology).
- Impaired cognitive control plays a role in schizophrenia, impulse control and anxiety disorders.



Dynamic Functional Connectivity Networks

- Functional connectivity networks transition through quasi-stationary microstates over time (Lehmann et al. 1997).
- Current Approaches to network state representations:
 - ▶ Sliding window FC analysis (Chang and Glover, 2010)
 - ▶ k-means clustering (Allen et al. 2012)
 - ▶ Principal Component Analysis (Leonardi et al. 2013)
- Shortcomings: The intrinsic network structure is not preserved: Averaging, Vectorizing.
- Our solution: Tensors are used to represent and summarize functional connectivity networks.



Outline

- 1 Introduction
- 2 Time-Frequency Phase Synchrony**
- 3 Tensor Subspace Analysis
- 4 State Representation
 - Subject Summarization
 - Time Summarization
- 5 Experimental Results
- 6 Conclusion and Future Work

Functional Connectivity: Phase Synchrony

- Reduced-interference Rihaczek distribution (RID-Rihaczek):

$$C_i(t, \omega) = \int \int \underbrace{\exp\left(-\frac{(\theta\tau)^2}{\sigma}\right)}_{\text{Choi-Williams kernel}} \underbrace{\exp(j\frac{\theta\tau}{2})}_{\text{Rihaczek kernel}} A_i(\theta, \tau) e^{-j(\theta t + \tau\omega)} d\tau d\theta. \quad (1)$$

▸ Ambiguity function: $A_i(\theta, \tau) = \int s_i(u + \frac{\tau}{2}) s_i^*(u - \frac{\tau}{2}) e^{j\theta u} du$.

- The phase distribution: $\Phi_i(t, \omega) = \arg \left[\frac{C_i(t, \omega)}{|C_i(t, \omega)|} \right]$.
- The phase difference between the two signals can be defined as: $\Phi_{(i,j)}^k(t, \omega) = |\Phi_i^k(t, \omega) - \Phi_j^k(t, \omega)|$.
- Phase locking value (PLV) quantifies the functional integration, as:

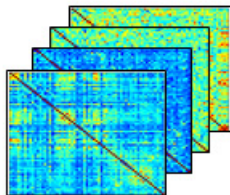
$$PLV_{(i,j)}(t, \omega) = \frac{1}{L} \left| \sum_{k=1}^L \exp(j\Phi_{(i,j)}^k(t, \omega)) \right|, \quad 0 \leq PLV \leq 1. \quad (2)$$

Construction of d-FCNs

- Functional connectivity matrix:

$$G_{s,(i,j)}(t) = \frac{1}{\Omega} \sum_{\omega=\omega_a}^{\omega_b} PLV_{s,(i,j)}(t, \omega), \quad (3)$$

- $G_{(i,j)}(t) \in [0, 1]$, $[\omega_a, \omega_b]$: frequency band of interest, Ω : the number of frequency bins, s : the subject.

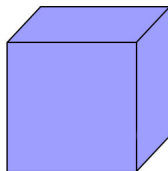


Outline

- 1 Introduction
- 2 Time-Frequency Phase Synchrony
- 3 Tensor Subspace Analysis**
- 4 State Representation
 - Subject Summarization
 - Time Summarization
- 5 Experimental Results
- 6 Conclusion and Future Work

Overview of tensors

- The extension of vectors and matrices to higher dimension is called multiway array, or tensor.
- $\mathcal{X} \in \mathbb{R}^{m_1 \times m_2 \times \dots \times m_d}$ is a d -way tensor, where $x_{i_1, i_2, i_3, \dots, i_d}$ is its $(i_1, i_2, i_3, \dots, i_d)$ th element.
- Collection of the FC matrices of all subjects, $\mathbf{G}_s(t)$, forms $\mathcal{G}(t) \in \mathbb{R}^{N \times N \times S}$.



Tucker Decomposition

- Tucker Decomposition is flexible in representing higher order data, and has orthogonal component matrices.
- Tucker decomposition is calculated using alternative least square (ALS) method.

Tucker decomposition of $\mathcal{X} \in \mathbb{R}^{m_1 \times m_2 \times \dots \times m_d}$:

$$\mathcal{X} = \mathcal{C} \times_1 \mathbf{U}^{(1)} \times_2 \mathbf{U}^{(2)} \times_3 \mathbf{U}^{(3)} \dots \times_d \mathbf{U}^{(d)} + \mathcal{E},$$

$$\mathcal{X} = \sum_{i_1, i_2, i_3, \dots, i_d} C_{i_1, i_2, i_3, \dots, i_d} \left(\mathbf{u}_{i_1}^{(1)} \circ \mathbf{u}_{i_2}^{(2)} \circ \mathbf{u}_{i_3}^{(3)} \circ \dots \circ \mathbf{u}_{i_d}^{(d)} \right) + \mathcal{E}_{i_1, i_2, i_3, \dots, i_d}, \quad (4)$$

- ▶ $\mathcal{C} \in \mathbb{R}^{r_1 \times r_2 \times \dots \times r_d}$ is the core tensor.
- ▶ $\mathbf{U}^{(1)} \in \mathbb{R}^{m_1 \times r_1}$, $\mathbf{U}^{(2)} \in \mathbb{R}^{m_2 \times r_2}$, \dots , $\mathbf{U}^{(d)} \in \mathbb{R}^{m_d \times r_d}$.
- ▶ $\mathcal{E} \in \mathbb{R}^{m_1 \times m_2 \times \dots \times m_d}$ is the residual.

Tucker Decomposition continued

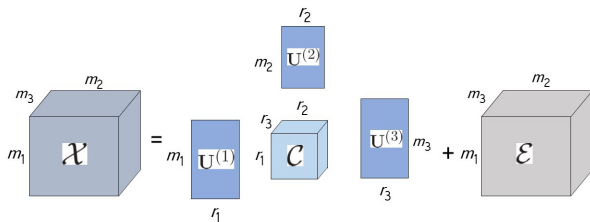


Figure: Tucker decomposition for a 3-way tensor.

n-mode product

n-mode product is multiplying the tensor unfolded along the n th mode by a matrix.

$$\mathcal{X} \times_n \mathbf{U} = \mathbf{U}^\dagger \mathbf{X}_{(n)} = \sum_{i_n} x_{i_1, i_2, \dots, i_n, \dots, i_d} U_{j_n, i_n} \quad (5)$$

Outline

- 1 Introduction
- 2 Time-Frequency Phase Synchrony
- 3 Tensor Subspace Analysis
- 4 State Representation**
 - Subject Summarization
 - Time Summarization
- 5 Experimental Results
- 6 Conclusion and Future Work

Overview

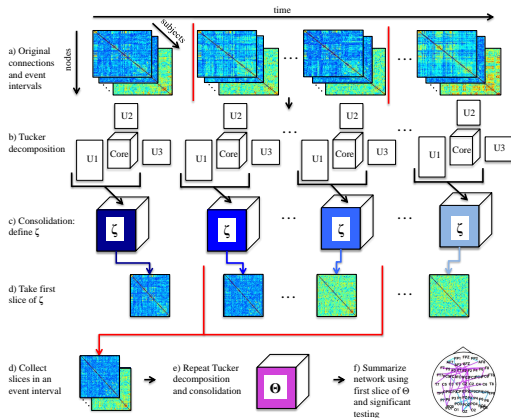


Figure: Functional connectivity state summarization algorithm flowchart.

Subject Summarization

- $\mathcal{G}(t) \in \mathbb{R}^{N \times N \times S}$ within the time interval $t = 1, 2, \dots, T$ is fully decomposed using Tucker decomposition:

$$\mathcal{G}(t) = \mathcal{C}(t) \times_1 \mathbf{U}^{(1)}(t) \times_2 \mathbf{U}^{(2)}(t) \times_3 \mathbf{U}^{(3)}(t). \quad (6)$$

- Let's define:

$$\zeta(t) = \mathcal{C}(t) \times_1 \mathbf{U}^{(1)}(t) \times_2 \mathbf{U}^{(2)}(t) \rightarrow \mathcal{G}(t) = \zeta(t) \times_3 \mathbf{U}^{(3)}(t).$$

- The subtensor $\theta(t) \in \mathbb{R}^{N \times N}$ captures most of the energy of the activation patterns across subjects at time:

$$\theta(t) = \zeta_{i_3=1}(t) = \sum_{s=1}^S U_{s,1}^{(3)}(t) \mathbf{G}_s(t). \quad (7)$$

Time Summarization

- $\theta(t)$, $\forall t \in \{1, 2, \dots, T\}$ are summarized across time mode to derive the state connectome.
- The 3-way tensor $\Theta \in \mathbb{R}^{N \times N \times T}$ is constructed from $\theta(t)$, and fully decomposed using Tucker decomposition:

$$\Theta = \vartheta \times_1 \bar{\mathbf{U}}^{(1)} \times_2 \bar{\mathbf{U}}^{(2)} \times_3 \bar{\mathbf{U}}^{(3)} = \bar{\zeta} \times_3 \bar{\mathbf{U}}^{(3)}. \quad (8)$$

- The subtensor $\eta = \bar{\zeta}_{i_3=1} = \sum_{t=1}^T \bar{U}_{t,1}^{(3)} \Theta_{i_3=t}$ captures the largest amount of energy across all time steps.

Significance Testing

- The significant edges of η is determined through hypothesis testing.
- A Gaussian distribution for the edge values in η is assumed.
- This assumption can be validated using Kolmogorov–Smirnov test.
- z-test is used on the edges of η to determine the most significant edges.

$$\mathbf{H}_0 : \eta(i, j) \sim \mathcal{N}_{erp}(\mu_{erp}, \sigma_{erp})$$

$$\mathbf{H}_1 : \eta(i, j) \sim \mathcal{N}_1(\mu_1 \neq \mu_{erp}, \sigma_1 \neq \sigma_{erp})$$

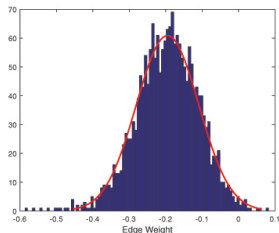


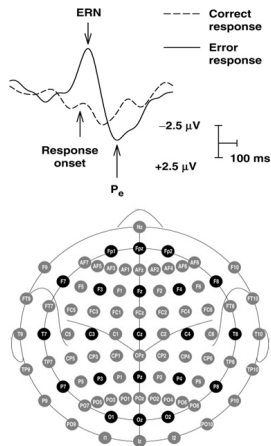
Figure: The histogram of the projected tensor edge values in the matrix η for ERN.

Outline

- 1 Introduction
- 2 Time-Frequency Phase Synchrony
- 3 Tensor Subspace Analysis
- 4 State Representation
 - Subject Summarization
 - Time Summarization
- 5 Experimental Results**
- 6 Conclusion and Future Work

EEG Data

- Error-Related Negativity (ERN) occurs 50-100ms after subjects made errors in response to a speeded motor task.
- Modified Eriksen flanker task for 2 seconds with multiple trials (10-40 error trials per subject).
- 91 subjects, 63 electrodes collected from undergraduates at the University of Minnesota.
- Sampling rate: 128 Hz.
- ERN is dominated by partial phase-locking of intermittent theta band (3-7 Hz) EEG activity between mPFC and IPFC (Cavanagh et al., 2009).



Experimental Results

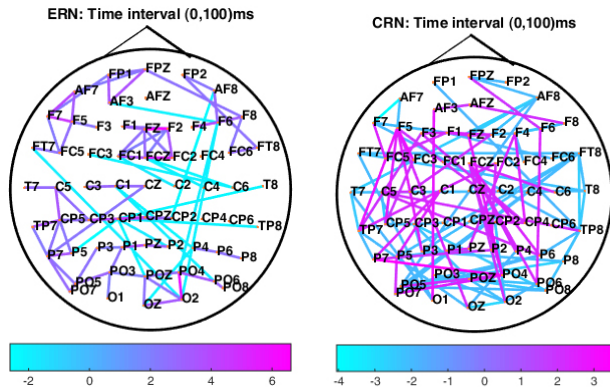


Figure: The most significant edges of the network summarization matrix, η with $p = 0.95$ for: (a) ERN, (b) CRN.

Experimental Results

Discussion

- ERN time interval:
 - ▶ Increased connectivity in medial- prefrontal regions, engaging electrodes (F1, Fz, F2, FC1, FCz, FC2) → Engagement of these regions during the ERN.
 - ▶ Sparse connections from right lateral frontal to parietal and occipital regions.
- CRN time interval:
 - ▶ Connectivity between right lateral frontal and left-temporal regions.
 - ▶ Strong connections between left lateral frontal and parietal region.

Outline

- 1 Introduction
- 2 Time-Frequency Phase Synchrony
- 3 Tensor Subspace Analysis
- 4 State Representation
 - Subject Summarization
 - Time Summarization
- 5 Experimental Results
- 6 **Conclusion and Future Work**

Summary

- We proposed a tensor based method for data reduction of dynamic functional connectivity matrices across subjects.
- Tensor-tensor projection along both directions can be used to summarize the connectivity within different time intervals.

Future Work

- Detect the change points instead of using *a priori* information to define time intervals.
- Extend this work to include the frequency information as the 5th mode of the tensor.